

Neutrino emission and initial evolution of axionic quark nuggets

Oswaldo P. Santillán ^{*}and Alejandro Morano [†]

Abstract

The axion quark nuggets introduced in [1]-[14] are a candidate for cold dark matter which, in addition, may be relevant in baryogenesis scenarios. The present letter studies the evolution of these objects till they enter in the colour superconducting phase. This evolution was already considered in [6] under the assumption that the baryon number at the domain wall surrounding the object is predominant, and that internal and external fluxes are not relevant. In the present work the possibility that a volume baryon number contribution is turned on and that the object may emit a large amount of neutrinos due to quark-antiquark annihilations is taken into account. This results into a more violent contraction of the object and perhaps a more effective cooling. Even taking into account these corrections, it is concluded that the cosmological applications of these objects are not spoiled. These applications are discussed along the text.

1. Introduction

One important problem in cosmology and particle physics is to understand if the present universe is baryon asymmetric or if the anti-baryons are segregated from baryons on very large scales. If there were galaxies of matter and anti matter in a given cluster of galaxies then, due to the presence of inter cluster gases, there should be nucleon anti-nucleon annihilations leading to strong γ ray emissions [15]. As this effect is not observed, and since galaxies like Virgo contains around $10^{14}M_{\odot}$ of matter, it is believed anti-matter should be segregated from matter on scales larger than $10^{14}M_{\odot}$. On the other hand, if the universe was initially baryon symmetric, then nucleons and anti-nucleons will freeze out at a temperature value $T \sim 22$ MeV. The ratio between the baryon number and the entropy densities that remains at this temperature is around nine orders of magnitude smaller than the observed value. This discrepancy may be avoided if there is an unknown segregation mechanism between baryons and anti-baryons which takes place at $T \sim 41$ MeV [15]. However, the Hubble horizon at these temperature is considerably smaller than $10^{14}M_{\odot}$. A possible solution is that the universe at $T \geq 41$ MeV was already in a baryon asymmetric state. There are particle physics scenarios which predict non zero baryon number [15], several of them are based on the Sakharov requirements for baryogenesis [16]-[17]. These requirements include in particular C and CP violation, and tiny baryon number violating interactions at the beginning of the universe.

Another possible explanation for baryogenesis was presented in [1]-[14]. This scenario is based on an apparently unrelated problem namely, the axion solution of the CP problem in QCD [18]-[21]. The axion is a pseudo scalar particle a that has several cosmological applications related to the formation of topological defects. An example are domain walls. At first sight, it is believed that such walls are problematic, as their evolution should overcome the critical energy density $\rho_c \sim 8.27 \cdot 10^{-27} \text{kg/m}^3$ which will lead to a catastrophe with observations, as discussed in [21] and references therein. But there exist the so called $N = 1$ axion models for which this problem does not exist, and there exist several ideas on how solving this problem for other types of axion models [21]. The authors of [1]-[14]

^{*}Instituto de Matemática Luis Santaló (IMAS), UBA CONICET, Buenos Aires, Argentina firenzecita@hotmail.com and osantil@dm.uba.ar.

[†]Departamento de Física, UBA, Buenos Aires, Argentina

assume that at a temperature $T \sim 100$ MeV there exists a network of domain walls described in terms of a Kibble-Zurek mechanism [22]-[23]. These domain walls admits non trivial quark configurations which, due non trivial asymptotic conditions, carry non zero baryon number [6]. Owing to the domain wall tension σ , some of these regions tends to contract and press the quark-gluon plasma trapped inside. As a consequence, the system acquires a non zero chemical potential μ and contracts until the internal Fermi pressure equals the external one, and then realises damped oscillations around the equilibrium radius R_e . The resulting internal temperature T_i is small enough, and the chemical potential μ is large enough, for reaching the colour superconducting (CS) phase in the bulk of the object [24]-[25]. It is important to emphasize that binding energy Δ characteristic of this state is large enough for these objects not participating in nucleosynthesis at $T \sim 1$ MeV [3].

The formation of the axion nuggets described above however, does not explain by itself the baryon asymmetry of the universe. Despite these objects contain net baryon or anti-baryon number, it is expected the presence of equal quantity of them if the underlying physics does contain baryon number violating processes. Thus, a further mechanism for asymmetry generation should be found. A crucial point for generating a larger number of anti-baryon objects may be the dynamics of the coherent axion field, which may lead to a preferential evolution in favor of anti nuggets. This mechanism is effective regardless the small value of the θ term as long as it remains coherent on the universe scale during the formation process [6]. This is a new feature, not present in the ordinary quark nuggets models such as [26]-[27]. These hypothesis are reasonable from the physical point of view. However, a precise quantitative analysis about the resulting asymmetry is technically involved and, at the moment, is lacking. There are other type of segregation mechanisms such as [28] for baryogenesis, but these will not be considered in the present letter.

There are some special features that distinguish axion quark nuggets from other dark matter candidates. First, these axion lumps are not supposed to be weakly interacting with ordinary matter. Their interaction is strong in fact, but they are macroscopically large as well. For this reason, the quotient between the cross section for interaction with visible baryons to their mass $\sigma/M \sim 10^{-10} \text{cm}^2/\text{g}$, which is well below the typical astrophysical limits $\sigma/M \sim \text{cm}^2/\text{g}$ [3]. Another salient characteristic is that these compact objects are long lived, with mean life time larger than the present age of the universe. In fact, it has been suggested that the excess of γ ray flux in MeV and GeV bands may be explained in terms of the rare annihilations between these objects and ordinary baryons. In addition, these objects interact noticeably with photons. However, the mean free time of photons when colliding with these objects is much larger than the Hubble time, thus these objects can be considered as cold dark matter, even when they are not electromagnetically neutral. These characteristics makes these objects different than, for instance, WIMPs. Further details are discussed in [3].

The evolution of these objects till they enter in the CS phase [24]-[25] was considered in [6]. In the present letter a variant for the dynamics of such objects is described. Although there are some different details about the nature of the formation in comparison with those pointed [6], the main cosmological applications remain valid. The main differences are the following. In studying the fate of the axion nuggets, the authors of [6] assume that the main contribution to the baryon number of the object is given by the wall contribution, and neglect the effect of internal and external fluxes. In the present letter it is assumed that, besides this surface contribution, a considerable volume baryon number appears. In fact, the CS phase is expected to appear in the bulk of the object at the time of formation. In addition, it is assumed that there is a considerable neutrino emission due to quark anti-quark annihilations. The neutrino emissivity plays the role of expulsion of fuel, and generates a violent contraction of the object. Even taking into account these circumstances, we are able to estimate that the object is formed when the universe temperature is around $T \sim 41$ MeV and that it falls into the CS phase. The internal temperature however, is not identified with the external one, as the neutrino emission may induce a considerable cooling. It should be emphasised that there are effects that are neglected, for instance neutrino or other particle adsorption. But even taking into account that we are employing the most unfriendly conditions and still being able of obtain plausible

results, the present scenario gives a hint that axion quark nuggets may be a candidate for both cold dark matter production and baryogenesis.

The present letter is organised as follows. In section 2, the general form of the equations of motion for these objects is described. In section 3 these equations are expressed through thermodynamical quantities such as internal temperature, chemical potential and the radius of the object. In section 4 the neutrino emission is estimated, by assuming that initially quark anti-quark annihilations play the leading important role at the initial evolution. In section 5 the fate of the nugget till it enters in the colour superconducting phase is described. Section 6 contains the discussions of the obtained results.

2. The generic equations of motion

The initial state of an axion quark nugget is an axion domain wall enclosing some finite volume region [1]-[14]. The exterior and interior are assumed to be in a quark-gluon plasma state, both with zero chemical potential [6]. The external region may fall into the hadron phase at some point during the evolution of the object, however, this will not affect significantly the following description. The initial temperature of the universe is approximately at $T_0 \sim 100 - 150$ MeV which, to the standard history of the universe, corresponds to a time $t \sim 10^{-4}$ s. The domain wall tension σ tends to contract the object, until the internal Fermi pressure equals the surface tension, and the wall then realises damped oscillations around the equilibrium position. There are quark degrees of freedom living on the wall, therefore these objects carry non trivial baryon number even when their chemical potential μ vanishes inside and outside. This can be briefly explained as follows. The equations of motion of a Dirac fermion Ψ on a domain wall solution can be derived from the lagrangian [6]

$$\mathcal{L} = i\bar{\Psi}[\gamma^\mu \partial_\mu - m e^{i[\theta(z) - \phi(z)]\gamma_5} - \mu\gamma_0]\Psi. \quad (2.1)$$

The fields $\theta(z)$ and $\phi(z)$ describe the axion and η' fields constituting the wall. Here the four dimensional problem has been reduced to a two dimensional one, with \hat{z} a unit vector normal to the surface of the wall. By neglecting the back reaction of the fermions on the domain wall, there exist non trivial fermion degrees of freedom $\Psi(z)$ that can live in the wall. These non trivial solutions carry a non zero baryon number

$$N = \int \bar{\Psi}\gamma_0\Psi dx^3, \quad (2.2)$$

a number that is non vanishing due to non trivial asymptotic [6].

The value of the QCD axion constant is believed to be in the range $10^9\text{GeV} < f_a < 10^{12}\text{GeV}$ [29]-[31]. The value to be employed here is close to $f_a \sim 10^{12}\text{GeV}$, which means that the axion mass is close to the value

$$m_a \sim \frac{m_\pi f_\pi}{f_a} \sim 10^{-5}\text{eV}. \quad (2.3)$$

This complements in some sense the results of [5], as this reference considers a value close to $f_a \sim 10^{10}\text{GeV}$. The relevant correlation length can be estimated as $\xi \sim m_a^{-1} \sim 1$ cm. If a Kibble-Zurek mechanism [22]-[23] is assumed to take place for domain walls, then the probability formation of regions of radius R is of the order $e^{-\frac{R^2}{\xi^2}}$, thus larger bubbles are exponentially suppressed. For this reason, it will be assumed that initial radius is of the order of $R_0 \sim 1$ cm. Neglecting the fermion backreaction, the surface tension acting inwards on the bubble is given by

$$\sigma \sim 8f_a m_\pi f_\pi \sim 10^{20}\text{MeV}^3, \quad (2.4)$$

for the choice of f_a given above.

The purpose of the present work is to understand qualitatively the fate of this region as it contracts. The equations of motion of the bubbles just described will be taken schematically as follows

$$\frac{dP_R^\alpha}{d\tau} + \frac{dP_\nu^\alpha}{d\tau} = F^\alpha, \quad (2.5)$$

with $\alpha = 0, 1, 2, 3$ and τ the proper time of the event. Equations of this type describe the motion of a relativistic rocket whose mass M varies with time due to the expulsion of fuel. The role of the fuel is played by the loss of neutrinos, whose momentum was denoted above by P_ν^α . In the last expression, P_R^α denotes the 4-momentum of an infinitesimal mass element dM composing the bubble. In addition, the 4-force acting on the system

$$F^\alpha = \frac{1}{\sqrt{1 - \dot{R}^2}}(f \cdot \dot{R}, f^i),$$

has been introduced. Here f^i being the force applied over the system, which is radially directed in the frame located at the center of the bubble. In practice, this force will be the sum of the surface tension force, and the one arising from the internal and external pressures. The bubble itself is considered as the sum of all these infinitesimal elements, simultaneously moving in the radial direction. The neutrinos are assumed to be emitted isotropically.

The equations written above are covariant, that is, they are valid in any inertial frame. The derivatives with respect to the proper time τ of the 4-vectors P^α in (2.5) can be related to a coordinate time t of the reference system located at the center of the bubble by

$$\frac{d}{d\tau} = \frac{1}{\sqrt{1 - \dot{R}^2}} \frac{d}{dt}.$$

The momentum of a surface element of the wall with respect to this reference system is

$$P_R^0 = \frac{dM}{\sqrt{1 - \dot{R}^2}}, \quad P_R^i = \frac{\dot{R}dM}{\sqrt{1 - \dot{R}^2}}.$$

The neutrino momentum is such that $(P_\nu^0)^2 = P_\nu^i P_\nu^i$ since it can be considered as a relativistic particle. The transformation of the momentum P_ν from frame of the wall to the momentum from center of the bubble P'_μ is given by

$$P'_\nu{}^\alpha = \sqrt{\frac{1 - \dot{R}}{1 + \dot{R}}} P_\nu^\alpha.$$

On the other hand

$$\frac{dP'_\nu{}^\alpha}{d\tau} = \frac{dP'_\nu{}^\alpha}{dP'_\nu{}^\beta} \frac{dP_\nu^\beta}{d\tau}.$$

By combining the last two formulas it is obtained that

$$\frac{dP'_\nu{}^\alpha}{d\tau} = \sqrt{\frac{1 - \dot{R}}{1 + \dot{R}}} \frac{dP_\nu^\beta}{d\tau}.$$

By integrating along the solid angle $d\Omega$ and by simplifying a common $\sqrt{1 - \dot{R}^2}$ factor, the equation (2.5) can be expressed as follows

$$\frac{d}{dt} \left(\frac{M}{\sqrt{1 - \dot{R}^2}} \right) + \sqrt{\frac{1 - \dot{R}}{1 + \dot{R}}} \frac{dP_\nu}{dt} = 4\pi R^2 \dot{R} \Delta P, \quad (2.6)$$

$$\frac{d}{dt} \left(\frac{M \dot{R}}{\sqrt{1 - \dot{R}^2}} \right) + \sqrt{\frac{1 - \dot{R}}{1 + \dot{R}}} \frac{dP_\nu}{dt} = 4\pi R^2 \Delta P. \quad (2.7)$$

These equations represent a variable mass nugget emitting neutrinos as fuel, and acted by radial forces. They will be supplemented below, when applies, with a further constraint arising from the conservation of the baryonic number of the system.

3. The explicit equations of movement

The emission of neutrinos is usually described in terms of the so called emissivity Q_ν [34]-[47] through the relation

$$\frac{dP_\nu}{dt} = \frac{4\pi R^3}{3} Q_\nu. \quad (3.8)$$

The emissivity Q_ν will be characterised in the next section. But at this point, it may be convenient to describe in detail the other quantities appearing in the equations (2.6)-(2.7). This system can be rewritten as follows

$$\frac{d}{dt} \left(\frac{M}{\sqrt{1-\dot{R}^2}} \right) + \sqrt{\frac{1-\dot{R}}{1+\dot{R}}} \frac{4\pi}{3} R^3 Q_\nu = 4\pi R^2 \dot{R} \Delta P, \quad (3.9)$$

$$\frac{M\ddot{R}}{\sqrt{1-\dot{R}^2}} + \left[4\pi R^2 \dot{R} \Delta P - \sqrt{\frac{1-\dot{R}}{1+\dot{R}}} \frac{4\pi}{3} R^3 Q_\nu \right] \dot{R} + \sqrt{\frac{1-\dot{R}}{1+\dot{R}}} \frac{4\pi}{3} R^3 Q_\nu = 4\pi R^2 \Delta P. \quad (3.10)$$

Note that the equation (3.9) is the same as (2.6). On the other hand, the equation (3.10) is obtained by (2.7) by replacing the derivative of $M(1-\dot{R}^2)^{-\frac{1}{2}}$ with respect to t through (2.6). Now, if the motion of the bubble is non relativistic, that is $\dot{R} \ll 1$, then these equations may be reduced to

$$\frac{dM}{dt} + \frac{4\pi}{3} R^3 Q_\nu = 4\pi R^2 \dot{R} \Delta P, \quad (3.11)$$

$$M\ddot{R} + \frac{4\pi}{3} R^3 Q_\nu = 4\pi R^2 \Delta P. \quad (3.12)$$

In order to solve these equations, the mass M and the pressure forces acting on the bubble should be characterised. In the following, it will be assumed that, during short periods, the state of the bubble may be approximated by an equilibrium state with well defined temperature T , chemical potential μ and internal pressure P_i . In this case, the mass M of the bubble is given by [6]

$$M = E = 4\pi R^2 \sigma + \frac{4\pi}{3} R^3 \rho + \frac{4\pi}{3} R^3 E_B \Theta(\mu - \mu_1) \left[1 - \frac{\mu_1^2}{\mu^2} \right], \quad E_B \sim (150 \text{ MeV})^4. \quad (3.13)$$

Here E_B is the bag constant, which should be taken into account when the chemical potential μ is higher than $\mu_1 \sim 330 \text{ MeV}$ [5]. The surface energy is sourced by the surface tension $\sigma \sim 8f_a m_\pi f_\pi$ of the axion wall. On the other hand, for generic fermions with mass m the pressure is related to the energy density ρ as follows

$$P = \frac{\rho}{3} - \frac{m^2 g}{6\pi^2} \int_m^\infty \frac{\sqrt{\epsilon^2 - m^2} d\epsilon}{e^{\frac{\epsilon - \mu}{T}} + 1}, \quad \rho = \frac{g}{2\pi^2} \int_m^\infty \frac{\epsilon^2 \sqrt{\epsilon^2 - m^2} d\epsilon}{e^{\frac{\epsilon - \mu}{T}} + 1}.$$

The last two formulas suggests that the pressure grows as m decreases. As the u and d quarks masses are of the order $m_u \sim m_d \sim 4 \text{ MeV}$ and the initial universe temperature is of the order $T_0 \sim 100 \text{ MeV}$, one may consider these quarks as massless. The s quark mass is $m_s \sim T_0$ and the pressure contribution of this species is smaller than the lighter counterparts. For this reason, the simplifying assumption that quark are massless will be employed when calculating some thermodynamical properties, as it will not lead to a significant deviation of their real values. Under this approximation, it follows that

$$P_q = \frac{1}{3} \rho - E_B \Theta(\mu - \mu_1) \left[1 - \frac{\mu_1^2}{\mu^2} \right], \quad \rho = \rho_q + \rho_{\bar{q}} = \frac{gT^4}{2\pi^2} \left[\int_0^\infty \frac{x^3 dx}{e^{x-\beta} + 1} + \int_0^\infty \frac{x^3 dx}{e^{x+\beta} + 1} \right], \quad \beta = \frac{\mu}{T},$$

with explicit result given by

$$P_q = \frac{1}{3} \left\{ \frac{7}{8} \frac{\pi^2 g T^4}{30} \left[1 + \frac{30\beta^2}{7\pi^2} + \frac{15\beta^4}{7\pi^4} \right] - 3E_B \Theta(\mu - \mu_1) \left[1 - \frac{\mu_1^2}{\mu^2} \right] \right\}. \quad (3.14)$$

Here the effect of the bag constant E_B has been included, which tends to decrease the pressure when it is turned on inside the compact object. In all the formulas derived above, the degeneracy g is

$$g = 4N_c N_f,$$

since there are 2 spin states and 2 charge states (particle and antiparticle) for any flavour and colour. In addition, the number of colours is $N_c = 3$. The external pressure, or universe pressure, is given by [6]

$$P_e = \frac{7}{8} \frac{\pi^2 g T_e^4}{90}, \quad T_e = T_0 \sqrt{\frac{t_0}{t}}, \quad T_0 \sim 100 - 150 \text{ MeV}, \quad t_0 \sim 10^{-4} \text{ sec.} \quad (3.15)$$

The pressure difference acting on the surface of the bubble is then

$$\Delta P = -\frac{2\sigma}{R} + \frac{7\pi^2 g T^4}{360} \left[1 + \frac{30\beta^2}{7\pi^2} + \frac{15\beta^4}{7\pi^4} \right] - \frac{7\pi^2 g T_e^4}{360} - E_B \Theta(\mu - \mu_1) \left[1 - \frac{\mu_1^2}{\mu^2} \right]. \quad (3.16)$$

Note that in the last formula the effect of the surface tension σ has been taken into account. In terms of the thermodynamical expressions found above, the equations (3.11)-(3.12) can be expressed as follows

$$\begin{aligned} \frac{d}{dt} \left[8\pi R^2 \sigma + \frac{2}{3} \frac{4\pi R^3}{3} \frac{7\pi^2 g T^4}{8 \cdot 30} \left(1 + \frac{30\mu^2}{7\pi^2 T^2} + \frac{15\mu^4}{7\pi^4 T^4} \right) + \frac{4\pi R^3}{3} \frac{7\pi^2 g T_e^4}{8 \cdot 90} + \frac{8\pi R^3}{3} E_B \Theta(\mu - \mu_1) \left(1 - \frac{\mu_1^2}{\mu^2} \right) \right] \\ + \frac{4\pi R^3}{3} \frac{d}{dt} \left[\frac{7\pi^2 g T^4}{8 \cdot 90} \left(1 + \frac{30\mu^2}{7\pi^2 T^2} + \frac{15\mu^4}{7\pi^4 T^4} \right) + E_B \Theta(\mu - \mu_1) \left(1 - \frac{\mu_1^2}{\mu^2} \right) \right] + \frac{4\pi}{3} R^3 Q_\nu = 0, \end{aligned} \quad (3.17)$$

$$\begin{aligned} \left[4\pi \sigma R^2 + \frac{4\pi R^3}{3} \frac{7\pi^2 g T^4}{8 \cdot 30} \left(1 + \frac{30\mu^2}{7\pi^2 T^2} + \frac{15\mu^4}{7\pi^4 T^4} \right) + \frac{4\pi R^3}{3} E_B \Theta(\mu - \mu_1) \left(1 - \frac{\mu_1^2}{\mu^2} \right) \right] \ddot{R} + \frac{4\pi}{3} R^3 Q_\nu \\ = -8\pi \sigma R + 4\pi R^2 \frac{7\pi^2 g T^4}{8 \cdot 90} \left(1 + \frac{30\mu^2}{7\pi^2 T^2} + \frac{15\mu^4}{7\pi^4 T^4} \right) - 4\pi R^2 E_B \Theta(\mu - \mu_1) \left(1 - \frac{\mu_1^2}{\mu^2} \right) - 4\pi R^2 \frac{7\pi^2 g T_e^4}{8 \cdot 90} + F_\eta. \end{aligned} \quad (3.18)$$

Here an additional force on the bubble F_η has been included which, at initial stages is not important. This is the QCD viscosity [32]

$$F_\eta = \eta R \dot{R},$$

which, for a contracting bubble, points outwards the surface of the bubble. This force is the result of several effects that occur during the contraction such as scattering of quarks, gluons and different Nambu-Goldstone bosons arising in different phases. The viscosity coefficient may depend on the temperature and chemical potential $\eta(T, \mu)$. The value $\eta \sim m_\pi^3 \sim 0.002 \text{ GeV}^3$ will be employed in the following [32]. However, a further knowledge of the behaviour of η as a function of T and μ is of course desirable, especially in the limit $\mu \gg T$.

The equations (3.17)-(3.18) constitute two equations for the three unknowns T , μ and R as functions of the time parameter t . The missing equation is related to the baryon number conservation of the system. The baryon number of the system for these bubbles is initially localised on the axionic wall and its approximate expression is

$$B = 4\pi N g R^2 \int \frac{d^2 p}{(2\pi)^2} \frac{1}{e^{\frac{\epsilon(p) - \mu}{T}} + 1}, \quad \epsilon = \sqrt{p^2 + m^2}. \quad (3.19)$$

Here N is given by the expression (2.2) and the wall was taken as a two dimensional object. These integrals, in the massless limit, can be expressed in terms of the variable ϵ by taking into account that $p dp = \epsilon d\epsilon$. The result is

$$B = 2N g R^2 T^2 \left[\text{Li}_2(-e^{-\frac{\mu}{T}}) + \frac{\pi^2}{6} + \frac{1}{2} \left(\frac{\mu}{T} \right)^2 \right]. \quad (3.20)$$

Since μ is positive, the argument z of the dilogarithm function $\text{Li}_2(z)$ is such that $|z| = e^{-\frac{\mu}{T}} < 1$. For this range of values, the dilogarithm may be expanded to give

$$B = 2NgR^2T^2 \left[\frac{\pi^2}{6} + \frac{1}{2} \left(\frac{\mu}{T} \right)^2 - \frac{\pi^2}{12} e^{-\frac{\mu}{T}} \right]. \quad (3.21)$$

However, as the chemical potential μ grows, a volume contribution is turned on. The baryon number must be corrected to

$$B = 2NgR^2T^2 \left[\frac{\pi^2}{6} + \frac{1}{2} \left(\frac{\mu}{T} \right)^2 - \frac{\pi^2}{12} e^{-\frac{\mu}{T}} \right] + \frac{4\pi R^3}{3} (n_f - \bar{n}_f),$$

where the last term is proportional to the difference between particles and anti-particles in a given volume. In the massless limit one has that

$$B = 2NgR^2T^2 \left[\frac{\pi^2}{6} + \frac{1}{2} \left(\frac{\mu}{T} \right)^2 - \frac{\pi^2}{12} e^{-\frac{\mu}{T}} \right] + \frac{2\pi g R^3 T^3}{9} \frac{\mu}{T} \left[1 + \frac{1}{\pi^2} \left(\frac{\mu}{T} \right)^2 \right]. \quad (3.22)$$

The baryon number conservation law is then expressed as

$$B = 2NgR^2T^2 \left[\frac{\pi^2}{6} + \frac{1}{2} \left(\frac{\mu}{T} \right)^2 - \frac{\pi^2}{12} e^{-\frac{\mu}{T}} \right] + \frac{2\pi g R^3 T^3}{9} \frac{\mu}{T} \left[1 + \frac{1}{\pi^2} \left(\frac{\mu}{T} \right)^2 \right] = \frac{Ng\pi^2}{3} R_0^2 T_0^2, \quad (3.23)$$

where T_0 and R_0 are the quantities at the beginning of the formation, and it is assumed that $\mu_0 = 0$. The equation (3.23) together with (3.17)-(3.18) constitute a system of three equations determining the temperature T , the chemical potential μ and the radius R of the object in terms of the initial conditions. In order to study the properties of their solutions, the expressions describing the emissivity Q_ν should be found. This will be done in the following section.

4. The neutrino momentum release

4.1 General emissivity formulas

As stated above, the neutrinos are assumed to be emitted isotropically due to pair annihilation in the bulk and at the border of the spherical region. The derivative of the momentum at a frame instantly at rest with respect to the domain wall is given in terms of the neutrino emissivity (3.8). For the emissivity, there are several channels to consider and there is extensive literature about the subject, with possible applications to neutron stars [34]-[47]. However, for high temperatures $T \gg \mu$ it will be assumed that quark-antiquark annihilation in two neutrinos $q + \bar{q} \rightarrow \nu + \bar{\nu}$ is the leading channel. The relevant coupling terms between the quarks and the neutrinos are given by

$$\mathcal{L}_{q\nu} = \frac{G_F}{\sqrt{2}} \left[\bar{\nu} \gamma^\mu \frac{1 + \gamma_5}{2} \nu \right] \left[\bar{u} \gamma^\mu (A_u + B_u \gamma_5) u + \bar{d} \gamma^\mu (A_d + B_d \gamma_5) d + \bar{s} \gamma^\mu (A_s + B_s \gamma_5) s \right],$$

where the following parameters

$$\begin{aligned} A_u &= \frac{1}{2} - \frac{4}{3} \sin^2 \theta_W, & B_u &= \frac{1}{2}, \\ A_d &= -\frac{1}{2} + \frac{2}{3} \sin^2 \theta_W, & B_d &= -\frac{1}{2}, \end{aligned} \quad (4.24)$$

have been introduced. The Weinberg angle θ_W is such that $\sin^2 \theta_W \sim 0.23$. We ignore the coupling for the s quarks, but we assume that they are smaller than for the light quarks. A discussion about this coupling will be given in the next section. By use of the above formulas the expression of the

emissivity may be found, which follows as a generalisation of the formula of electron emissivity [47] adapted to quarks. For instance, the emissivity for a given quark u is calculated by means of the following formula [47]

$$Q_u \sim \frac{G_F^2 m_u^9}{36\pi} \left\{ A_{u+}^2 \left[8(\Phi_{1u}U_{2u} + \Phi_{2u}U_{1u}) - 2(\Phi_{-1u}U_{2u} + \Phi_{2u}U_{-1u}) + 7(\Phi_{0u}U_{1u} + \Phi_{1u}U_{0u}) \right. \right. \\ \left. \left. + 5(\Phi_{0u}U_{-1u} + \Phi_{-1u}U_{0u}) \right] + 9A_{u-}^2 \left[\Phi_{0u}(U_{1u} + U_{-1u}) + U_{0u}(\Phi_{1u} + \Phi_{-1u}) \right] \right\}, \quad (4.25)$$

up to a factor related to colour matrices which is not far to unity. In the last expression, the following thermodynamical integrals

$$U_{ku} = \frac{1}{\pi^2} \int_0^\infty \frac{p_u^2 dp_u}{m_u^3} \left(\frac{\epsilon_u}{m_u} \right)^k f_u, \quad \Phi_{ku} = \frac{1}{\pi^2} \int_0^\infty \frac{p_u^2 dp_u}{m_u^3} \left(\frac{\epsilon_u}{m_u} \right)^k f_{\bar{u}}, \quad (4.26)$$

and the following parameters

$$A_{+u}^2 = A_u^2 + B_u^2, \quad A_{-u}^2 = A_u^2 - B_u^2,$$

have been introduced. Here

$$f_u = \frac{1}{e^{\frac{\epsilon_u - \mu_u}{T}} + 1}, \quad f_{\bar{u}} = \frac{1}{e^{\frac{\epsilon_u + \mu_u}{T}} + 1}.$$

Note that the difference between Φ_{ku} and U_{ku} is due to the sign of the chemical potential μ_u . Analogous expressions are true for d and s quarks.

When the density is high enough, $\mu \gg T$ the emissivity described above may not be the leading term anymore. A possible energy loss process is due to the beta quark decay $u + e^- \rightarrow d + \nu_e$ or $d \rightarrow e^- + u + \bar{\nu}_e$. The neutrino emissivity in this case is given by the well known Iwamoto formula [34]

$$Q_\nu = \frac{914}{315} G_f^2 \cos^2 \theta_c \mu_\mu \mu_d \mu_e \alpha_s T^6.$$

Here the Cabbibo angle θ_c is such that $\cos^2 \theta_c \sim 0.948$ and the condition of β equilibrium is

$$\mu_u = \mu_d + \mu_e, \quad \mu_s = \mu_d + \mu_e.$$

For high densities, the following approximation is valid

$$\mu_\mu = \mu_d, \quad \mu_e = 3^{\frac{1}{3}} Y_e^{\frac{1}{3}} \mu_u,$$

where the number Y_e for dense matter varies from $Y_e \sim 10^{-2}$ to $Y_e \sim 10^{-1}$. In these terms the emissivity is given by

$$Q_\nu = \frac{914}{315} G_f^2 \mu^3 Y_e^{\frac{1}{3}} \alpha_s T^6. \quad (4.27)$$

There are other neutrino processes for matter at high densities that can be effective for cooling, examples can be seen in the references [34]-[47] and [48]-[55]. It is important to remark that the formula (4.27) does not assume that the CS phase takes place. In fact, there are phases of matter which are not represented as a quark-gluon plasma for which the emissivity may be strongly suppressed, examples are given in [55]. In the following, it will be assumed that in the CS phase, the emissivity is very small in comparison with the afore mentioned processes.

4.2 An estimation of the emissivities

The study of the emissivity Q_ν given in (4.25) requires an estimation of the integrals (4.26). These integrals are all of the form

$$I_k = \frac{1}{m^{k+3}\pi^2} \int_0^\infty \frac{\epsilon^k p^2 dp}{1 + \exp(\frac{\epsilon - \mu}{T})},$$

where the chemical potential μ can take positive and negative values and $k = 2, 1, 0, -1$. As $\epsilon = \sqrt{p^2 + m^2}$ for relativistic particles, it follows that

$$p^2 dp = \epsilon \sqrt{\epsilon^2 - m^2} d\epsilon \sim \epsilon^2 \left(1 - \frac{m^2}{2\epsilon^2} - \frac{m^4}{8\epsilon^4}\right) d\epsilon.$$

The integrals under consideration are then given by

$$I_k = \frac{1}{m^{k+3}\pi^2} \int_m^\infty \frac{\epsilon^{k+1} \sqrt{\epsilon^2 - m^2} d\epsilon}{1 + \exp(\frac{\epsilon - \mu}{T})} \simeq \frac{1}{m^{k+3}\pi^2} \int_m^\infty \frac{\epsilon^{k+2} d\epsilon}{1 + \exp(\frac{\epsilon - \mu}{T})} \left(1 - \frac{m^2}{2\epsilon^2} - \frac{m^4}{8\epsilon^4}\right).$$

Consider first the case $k = 2$. The corresponding integral

$$I_2 \simeq \frac{1}{m^5\pi^2} \int_m^\infty \frac{\epsilon^4 d\epsilon}{1 + \exp(\frac{\epsilon - \mu}{T})} \left(1 - \frac{m^2}{2\epsilon^2} - \frac{m^4}{8\epsilon^4}\right),$$

can be found explicitly, the result is

$$\begin{aligned} I_2 \sim \frac{-1}{m^5\pi^2} \left[24T^5 \text{Li}_5(-e^{\frac{\mu-m}{T}}) + 24T^4 m \text{Li}_4(-e^{\frac{\mu-m}{T}}) + 12T^3 m^2 \text{Li}_3(-e^{\frac{\mu-m}{T}}) + 4T^2 m^3 \text{Li}_2(-e^{\frac{\mu-m}{T}}) \right. \\ \left. - Tm^4 \log(e^{\frac{\mu-m}{T}} + 1) \right] + \frac{1}{2m^3\pi^2} \left[2T^3 \text{Li}_3(-e^{\frac{\mu-m}{T}}) + 2T^2 m \text{Li}_2(-e^{\frac{\mu-m}{T}}) - Tm^2 \log(e^{\frac{\mu-m}{T}} + 1) \right] \\ + \frac{1}{8\pi^2 m} [m - T \log(e^{\frac{\mu}{T}} + e^{\frac{m}{T}})]. \end{aligned} \quad (4.28)$$

Here the polylogarithm functions

$$\text{Li}_{1+s}(x) = \frac{1}{\Gamma(s+1)} \int_0^\infty \frac{xk^s dk}{e^k - x}, \quad (4.29)$$

have been introduced.

Unlike the previous case, the integrals corresponding to $k = 1, 0, -1$ are not explicit. For dealing with them, the following approximated scheme will be employed. Consider the case $k = 1$ namely

$$I_1 \simeq \frac{1}{m^4\pi^2} \int_m^\infty \frac{\epsilon^3 d\epsilon}{1 + \exp(\frac{\epsilon - \mu}{T})} \left(1 - \frac{m^2}{2\epsilon^2} - \frac{m^4}{8\epsilon^4}\right).$$

The first two terms can be integrated explicitly but, to the best of our knowledge, there is no primitive for the last one. However, if one separates the last term and write the last expression as

$$I_1 \simeq \frac{1}{m^4\pi^2} \int_m^\infty \frac{\epsilon^3 d\epsilon}{1 + \exp(\frac{\epsilon - \mu}{T})} \left(1 - \frac{m^2}{2\epsilon^2}\right) - \frac{1}{\pi^2} \int_m^\infty \frac{d\epsilon}{1 + \exp(\frac{\epsilon - \mu}{T})} \frac{1}{8\epsilon},$$

then, by further making the variable change $\epsilon = T \log \eta$ one obtains

$$I_1 \simeq \frac{1}{m^4\pi^2} \int_m^\infty \frac{\epsilon^3 d\epsilon}{1 + \exp(\frac{\epsilon - \mu}{T})} \left(1 - \frac{m^2}{2\epsilon^2}\right) - \frac{e^{\frac{\mu}{T}}}{8\pi^2} \int_{e^{\frac{\mu}{T}}}^\infty \frac{d\eta}{\eta(e^{\frac{\mu}{T}} + \eta)} \frac{1}{\log \eta}.$$

The last integral can be successively be approximated by separating the cases $\mu < m$ or $\mu > m$. For instance, if $\mu < m$ the integrand can be expanded in terms of $e^{\frac{\mu}{T}}/\eta$ by use of geometric series, the result is

$$I_1 \simeq \frac{1}{m^4 \pi^2} \int_m^\infty \frac{\epsilon^3 d\epsilon}{1 + \exp(\frac{\epsilon - \mu}{T})} \left(1 - \frac{m^2}{2\epsilon^2}\right) - \frac{e^{\frac{\mu}{T}}}{8\pi^2} \int_{e^{\frac{\mu}{T}}}^\infty \frac{d\eta}{\eta^2 \log \eta} \left[1 - \frac{e^{\frac{\mu}{T}}}{\eta} + \frac{e^{\frac{2\mu}{T}}}{\eta^2}\right] \quad \text{for} \quad \mu < m.$$

In the other possible situation namely $\mu > m$ there are two η regions to consider, the first corresponds to $\epsilon < \mu$ and the second to $\epsilon > \mu$. In the first region the expansion parameter is $\eta/e^{\frac{\mu}{T}}$ and in the second $e^{\frac{\mu}{T}}/\eta$. The resulting integral is

$$I_1 \simeq \frac{1}{m^4 \pi^2} \int_m^\infty \frac{\epsilon^3 d\epsilon}{1 + \exp(\frac{\epsilon - \mu}{T})} \left(1 - \frac{m^2}{2\epsilon^2}\right) - \frac{e^{\frac{\mu}{T}}}{8\pi^2} \int_{e^{\frac{\mu}{T}}}^\infty \frac{d\eta}{\eta^2 \log \eta} \left[1 - \frac{e^{\frac{\mu}{T}}}{\eta} + \frac{e^{\frac{2\mu}{T}}}{\eta^2}\right] \\ - \frac{1}{8\pi^2} \int_{e^{\frac{\mu}{T}}}^{\frac{\mu}{m}} \frac{d\eta}{\eta \log \eta} \left[1 - \frac{\eta}{e^{\frac{\mu}{T}}} + \frac{\eta^2}{e^{\frac{2\mu}{T}}}\right], \quad \text{for}, \quad \mu > m.$$

The resulting integrals are explicit, the result is

$$I_1 \sim \frac{-1}{m^4 \pi^2} \left[6T^4 \text{Li}_4(-e^{\frac{\mu-m}{T}}) + 6T^3 m \text{Li}_3(-e^{\frac{\mu-m}{T}}) + 3T^2 m^2 \text{Li}_2(-e^{\frac{\mu-m}{T}}) - Tm^3 \log(e^{\frac{\mu-m}{T}} + 1)\right] \\ + \frac{1}{2m^2 \pi^2} \left[T^2 \text{Li}_2(-e^{\frac{\mu-m}{T}}) - Tm \log(e^{\frac{\mu-m}{T}} + 1)\right] + \frac{1}{8\pi^2} \left[e^{\frac{\mu}{T}} \text{Ei}\left(-\frac{m}{T}\right) - e^{\frac{2\mu}{T}} \text{Ei}\left(-\frac{2m}{T}\right) + e^{\frac{3\mu}{T}} \text{Ei}\left(-\frac{3m}{T}\right)\right], \quad (4.30)$$

for $\mu < m$ and

$$I_1 \sim \frac{-1}{m^4 \pi^2} \left[6T^4 \text{Li}_4(-e^{\frac{\mu-m}{T}}) + 6T^3 m \text{Li}_3(-e^{\frac{\mu-m}{T}}) + 3T^2 m^2 \text{Li}_2(-e^{\frac{\mu-m}{T}}) - Tm^3 \log(e^{\frac{\mu-m}{T}} + 1)\right] \\ + \frac{1}{2m^2 \pi^2} \left[T^2 \text{Li}_2(-e^{\frac{\mu-m}{T}}) - Tm \log(e^{\frac{\mu-m}{T}} + 1)\right] + \frac{1}{8\pi^2} \left[e^{\frac{\mu}{T}} \text{Ei}\left(-\frac{\mu}{T}\right) - e^{\frac{2\mu}{T}} \text{Ei}\left(-\frac{2\mu}{T}\right) + e^{\frac{3\mu}{T}} \text{Ei}\left(-\frac{3\mu}{T}\right)\right] \\ + \frac{1}{8\pi^2} \left[e^{-\frac{2\mu}{T}} \text{Ei}\left(\frac{2m}{T}\right) - e^{-\frac{\mu}{T}} \text{li}(e^{\frac{m}{T}}) + \log\left(\frac{m}{\mu}\right) - e^{-\frac{2\mu}{T}} \text{Ei}\left(\frac{2\mu}{T}\right) + e^{-\frac{\mu}{T}} \text{li}(e^{\frac{\mu}{T}})\right], \quad (4.31)$$

for $\mu > m$. In the above expressions the exponential integral function

$$\text{Ei}(x) = - \int_{-x}^\infty \frac{e^{-t} dt}{t}, \quad (4.32)$$

and the logarithmic integral

$$\text{li}(x) = - \int_0^x \frac{dt}{\log t}, \quad \text{for } x < 1, \quad \text{li}(x) = -\text{PV} \int_0^x \frac{dt}{\log t}, \quad \text{for } x > 1. \quad (4.33)$$

were introduced. Here PV denotes the Cauchy principal value, and $x = 1$ is a singular value.

The remaining integrals $k = 0, -1$ can be approximated by exactly the same method. Without quoting the details, the result is

$$I_0 \sim \frac{-1}{m^3 \pi^2} \left[2T^3 \text{Li}_3(-e^{\frac{\mu-m}{T}}) + 2T^2 m \text{Li}_2(-e^{\frac{\mu-m}{T}}) - Tm^2 \log(e^{\frac{\mu-m}{T}} + 1)\right] + \frac{1}{2m\pi^2} [m - T \log(e^{\frac{\mu}{T}} + e^{\frac{m}{T}})] \\ - \frac{m}{8\pi^2 T} \left[e^{\frac{\mu}{T}} \text{Ei}\left(-\frac{m}{T}\right) - 2e^{\frac{2\mu}{T}} \text{Ei}\left(-\frac{2m}{T}\right) + 3e^{\frac{3\mu}{T}} \text{Ei}\left(-\frac{3m}{T}\right)\right] - \frac{1}{8\pi^2} \left[e^{\frac{\mu-m}{T}} - e^{\frac{2\mu-2m}{T}} + e^{\frac{3\mu-3m}{T}}\right], \quad (4.34)$$

$$\begin{aligned}
I_{-1} \sim & \frac{-1}{m^2\pi^2} [T^2 \text{Li}_2(-e^{\frac{\mu-m}{T}}) - Tm \log(e^{\frac{\mu-m}{T}} + 1)] + \frac{1}{2\pi^2} \left[e^{\frac{\mu}{T}} \text{Ei}\left(-\frac{m}{T}\right) - e^{\frac{2\mu}{T}} \text{Ei}\left(-\frac{2m}{T}\right) + e^{\frac{3\mu}{T}} \text{Ei}\left(-\frac{3m}{T}\right) \right] \\
& + \frac{m^2}{8T^2\pi^2} \left[\frac{e^{\frac{\mu}{T}}}{2} \text{Ei}\left(-\frac{m}{T}\right) - 2e^{\frac{2\mu}{T}} \text{Ei}\left(-\frac{2m}{T}\right) + \frac{9}{2} e^{\frac{3\mu}{T}} \text{Ei}\left(-\frac{3m}{T}\right) \right] + \frac{m}{8T\pi^2} \left[\frac{1}{2} e^{\frac{\mu-m}{T}} - e^{\frac{2\mu-2m}{T}} + \frac{3}{2} e^{\frac{3\mu-3m}{T}} \right] \\
& + \frac{1}{16\pi^2} \left[-e^{\frac{\mu-m}{T}} + e^{\frac{2\mu-2m}{T}} - e^{\frac{3\mu-3m}{T}} \right], \tag{4.35}
\end{aligned}$$

for $\mu < m$ and

$$\begin{aligned}
I_0 \sim & \frac{-1}{m^3\pi^2} \left[2T^3 \text{Li}_3(-e^{\frac{\mu-m}{T}}) + 2T^2 m \text{Li}_2(-e^{\frac{\mu-m}{T}}) - Tm^2 \log(e^{\frac{\mu-m}{T}} + 1) \right] + \frac{1}{2m\pi^2} [m - T \log(1 + e^{\frac{m-\mu}{T}})] \\
& - \frac{m}{8\pi^2 T} \left[e^{\frac{\mu}{T}} \text{Ei}\left(-\frac{\mu}{T}\right) - 2e^{\frac{2\mu}{T}} \text{Ei}\left(-\frac{2\mu}{T}\right) + 3e^{\frac{3\mu}{T}} \text{Ei}\left(-\frac{3\mu}{T}\right) \right] + \frac{m}{8\pi^2 T} \left[2e^{-\frac{2\mu}{T}} \text{Ei}\left(\frac{2m}{T}\right) \right. \\
& \left. - 2e^{-\frac{2\mu}{T}} \text{Ei}\left(\frac{2\mu}{T}\right) + e^{-\frac{\mu}{T}} \text{li}(e^{\frac{\mu}{T}}) - e^{-\frac{\mu}{T}} \text{li}(e^{\frac{m}{T}}) \right] + \frac{1}{8\pi^2} [1 - e^{\frac{m-\mu}{T}} + e^{\frac{2m-2\mu}{T}}], \tag{4.36}
\end{aligned}$$

$$\begin{aligned}
I_{-1} \sim & \frac{-1}{m^2\pi^2} [T^2 \text{Li}_2(-e^{\frac{\mu-m}{T}}) - Tm \log(e^{\frac{\mu-m}{T}} + 1)] + \frac{1}{2\pi^2} \left[e^{\frac{\mu}{T}} \text{Ei}\left(-\frac{\mu}{T}\right) - e^{\frac{2\mu}{T}} \text{Ei}\left(-\frac{2\mu}{T}\right) + e^{\frac{3\mu}{T}} \text{Ei}\left(-\frac{3\mu}{T}\right) \right] \\
& + \frac{m^2}{8T^2\pi^2} \left[\frac{e^{\frac{\mu}{T}}}{2} \text{Ei}\left(-\frac{\mu}{T}\right) - 2e^{\frac{2\mu}{T}} \text{Ei}\left(-\frac{2\mu}{T}\right) + \frac{9}{2} e^{\frac{3\mu}{T}} \text{Ei}\left(-\frac{3\mu}{T}\right) \right] + \frac{1}{2\pi^2} \left[e^{-\frac{2\mu}{T}} \text{Ei}\left(\frac{2m}{T}\right) - e^{-\frac{\mu}{T}} \text{li}(e^{\frac{m}{T}}) \right. \\
& + \log\left(\frac{m}{\mu}\right) - e^{-\frac{2\mu}{T}} \text{Ei}\left(\frac{2\mu}{T}\right) + e^{-\frac{\mu}{T}} \text{li}(e^{\frac{\mu}{T}}) \left. \right] + \frac{m^2}{8\pi^2 T^2} \left[-2e^{-\frac{2\mu}{T}} \text{Ei}\left(\frac{2\mu}{T}\right) + 2e^{-\frac{2\mu}{T}} \text{Ei}\left(\frac{2m}{T}\right) + \frac{e^{-\frac{\mu}{T}}}{2} \text{li}(e^{\frac{\mu}{T}}) \right. \\
& \left. - \frac{e^{-\frac{\mu}{T}}}{2} \text{li}(e^{\frac{m}{T}}) \right] + \frac{3m^2}{16\pi^2 T\mu\pi^2} - \frac{1}{16\pi^2} (1 - e^{\frac{m-\mu}{T}} + e^{\frac{2m-2\mu}{T}}) + \frac{m}{16\pi^2 T} (e^{\frac{m-\mu}{T}} - 2e^{\frac{2m-2\mu}{T}}). \tag{4.37}
\end{aligned}$$

for $\mu > m$. In these terms the emissivities (4.25) can be calculated by identifying Φ_k with I_k with $\mu < 0 < m$ and U_k with one of the I_k depending if $\mu > m$ or $\mu < m$.

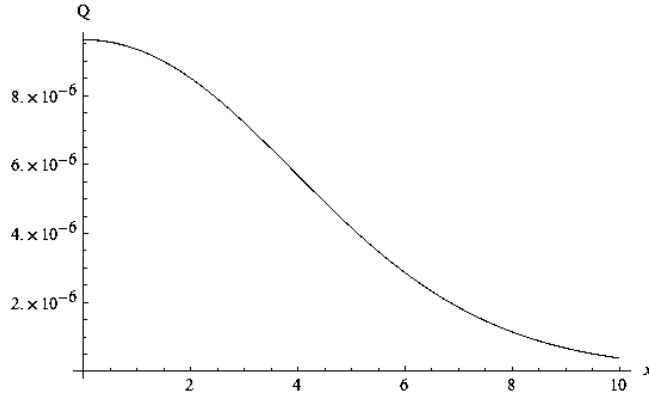


Figure 1: The massless limit of Q as a function of $x = \mu/T$ for $T = 100$ MeV. The units in all the figures are MeV^5 .

The formulas (4.28)-(4.37) are approximated to a given order. However the massless limit $m \rightarrow 0$ is exact. In the massless regime the emissivities (4.25) are given by

$$Q \sim \frac{32G_f^2 T^9}{\pi^5} A_{u+}^2 [\text{Li}_5(-e^{\frac{\mu}{T}}) \text{Li}_4(-e^{-\frac{\mu}{T}}) + \text{Li}_5(-e^{-\frac{\mu}{T}}) \text{Li}_4(-e^{\frac{\mu}{T}})]. \tag{4.38}$$

As the figure 1 shows, this function is bell shaped and has values that run from 10^{-5} MeV^5 to 8.10^{-6} MeV^5 for $T \sim 100 \text{ MeV}$ and $0 < \mu < 10 \text{ T}$. The units of the figures are all MeV^5 . In addition, for $\mu \rightarrow \infty$ and T fixed it goes to zero. This makes sense, as the excess of particles over anti-particles

$$n_q - n_{\bar{q}} \sim \frac{\mu}{T} \left[1 + \frac{\mu^2}{\pi^2 T^2} \right],$$

is very large in this limit, so annihilation is likely to be suppressed. It is interesting to analyse how the

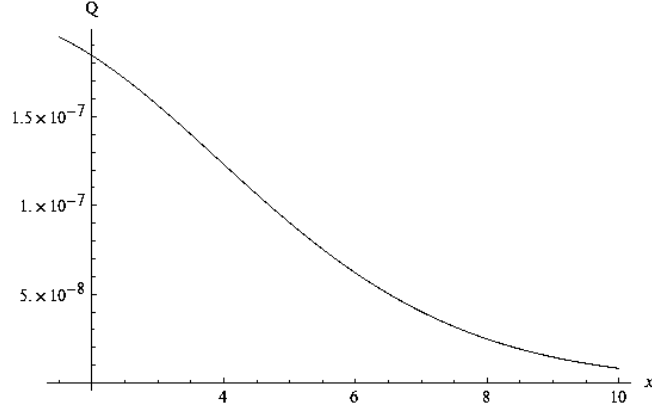


Figure 2: The values of Q for $m \sim m_u$ and $T = 100 \text{ MeV}$ as a function of $x = \mu/T$.

emissivity varies as a function of the quark mass m . It is not clear at first sight if the emissivity would grow or decay when m increases, since the density of heavier particles is suppressed by a Fermi-Dirac factor but its decay rate seems to increase with the mass. At the end, it is expected that $Q \rightarrow 0$ when

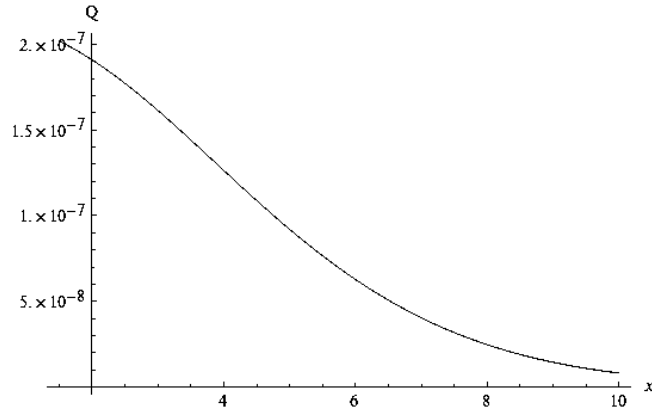


Figure 3: The values of Q for $m \sim m_s$ and $T = 100 \text{ MeV}$ as a function of $x = \mu/T$.

$m \rightarrow \infty$, as such a massive quark is likely to decay fast but it is strongly suppressed by thermodynamics. The exponential integral $\text{Ei}(-x)$ is such that $\text{Ei}(-x) \rightarrow \infty$ when $x \rightarrow 0$. However, $x^\alpha \text{Ei}(-x) \rightarrow 0$ in this limit. In addition $x^\alpha \text{Ei}(-x) \rightarrow 0$ when $x \rightarrow \infty$ and $\alpha \geq 1$. The same result is true for the logarithm or polylogarithm terms appearing in (4.30)-(4.37). By use of these facts, one may obtain

that

$$\lim_{m \rightarrow \infty} Q(m, \mu, T) \rightarrow 0.$$

This is the expected result. On the other hand, there is an essential singularity when $\mu \rightarrow \infty$ and $m \rightarrow \infty$, since the behaviour of Q depends on the curve $(m(t), \mu(t))$ chosen for taking the limit.

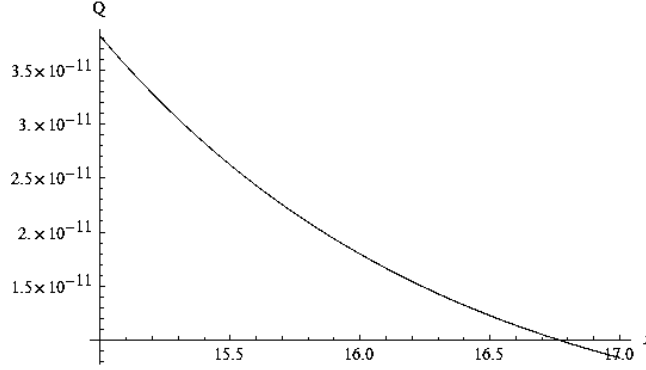


Figure 4: The values of Q for a very massive quark with mass $m \sim 10m_s$ and $T = 100$ MeV as a function of $x = \mu/T$ in the range $15 < x < 20$. Its values are never negative.

The conclusion given above related to the asymptotic behaviour of Q with respect to the mass however, does not give relevant information for moderate values of m such as $m \sim T$ or $m \sim m_u \sim m_d$. These moderate values are the ones relevant for the present work. In order to understand the behaviour of emissivity for these mass values, a numerical estimation is in order. We have plotted with Mathematica the emissivity in several regimes. We collect here some relevant cases for illustrative purposes. Figure 2 shows that for a light quark with mass m_u the emissivity is not considerably deviated from the massless case of figure 1. Figure 3 shows that for a quark of mass $m_s \sim T$ the deviation is also not very significant. We have plotted the emissivities for other temperatures and we have found a similar behaviour. A significant variation appears when the quark mass m is considerably larger than the temperature T , as figure 4 shows. In this case the emissivity gets significantly suppressed. Our results suggest that the emissivities for particles with masses below or of the order of the temperature T are more or less similar, but when the mass $m \gg T$ then Q starts to decrease considerably. The emissivities plotted above are all related to the case $\mu > m$, but in the other regime a similar conclusion applies. For this reason, for the present problem in consideration, the massless emissivity will be considered. In other words, the emissivity will be given by

$$Q \sim \frac{96G_f^2 T^9}{\pi^5} F\left(\frac{\mu}{T}\right), \quad (4.39)$$

with $F(x)$ a function taking values between 1 and 0.1 when $0 < x < 10$.

5. Description of the evolution of the bubble

After the emissivity has been characterised, the next section is to describe qualitatively the evolution of the bubble by use of the baryon number conservation condition (3.23) together with the equations of motion (3.17)-(3.18). As discussed in section 2, the initial radius is assumed to be of order $R_0 \sim 1$ cm. In addition, the small choice $N \sim 1 - 10$ in (3.23) will be employed. This corresponds to a baryon number $B \sim 10^{28} - 10^{29}$ for the object. For radius $R < 1$ cm and temperatures $T < 100$ MeV the

terms proportional to σR predominate over the ones proportional to $R^2 T^4$, and the emissivity Q_ν is even smaller. The difference becomes more accentuated as the radius or the temperature decreases. This means that the surface tension σ plays a major role in contracting the object initially. This situation, as discussed below, is reversed when the chemical potential reaches values $\mu \gg T$.

If initially the chemical potential $\mu = 0$, then the term proportional to R^3 in (3.23) vanishes. However, by taking into account that $T_0 \sim 100$ MeV it is seen that $R_0 T_0 \sim 10^{13}$. This suggests that the volume term in (3.23), which is proportional to $R^3 T^2 \mu$ may quickly starts to predominate over the surface term proportional to $R^2 T^2$, even when $\mu \ll T$. This follows from the fact that $N \sim 1 - 10$ is considerably smaller than $R_0 T_0 \sim 10^{13}$. Now, in the regime $\mu \ll T$ it may be assumed in (3.17) that

$$1 + \frac{30\mu^2}{7\pi^2 T^2} + \frac{15\mu^4}{7\pi^4 T^4} \sim 1. \quad (5.40)$$

This does not mean that the time derivatives of these quantities are small, since even a small function may have a large slope at some point. But if it is supposed that the slope is moderate then equation (3.17) implies that

$$\frac{28\pi^3 g T^3}{270} \dot{T} + \frac{4\pi}{3} Q_\nu \geq 0.$$

This follows from the fact that the first term in (3.17) is assumed to be negative. This is justified because the surface tension term proportional σ is large in comparison with the other components of the pressure, for a radius smaller than a centimeter. Thus it may be assumed safely that the bubble is initially contracting and perhaps cooling, which means that the derivatives of all these terms are all negative. By use of (4.38) and the numerical values of the emissivity found in the previous section, the last equation integrates approximately to

$$T \geq \frac{T_0}{\left[1 + 10^{10} \left(\frac{t}{s}\right)\right]^{\frac{1}{5}}}.$$

Here the functional form (4.39) the value $G_f \sim 10^{-5} \text{GeV}^{-2}$ were taken into account, and the chemical potential μ in (4.38) was set to zero for simplicity.

The last formula shows that, for the temperature to lower down to $T = T_0/3$, at least a time $t \sim 10^{-9}$ s is required, irrespective to the initial temperature value T_0 . This is exactly the time if no contraction takes place, that is, for constant R . For decreasing R this value may be larger. However, we will assume that this is the characteristic time such that, for $t \leq 10^{-9}$ s, the temperature remains constant and after that, a considerable cooling starts due to the neutrino emission. Note that the external temperature (3.15) will be also constant for such short time period. In the present scheme, there is no identification between the temperature T of the object and the external temperature T_e . This line of reasoning may not be true when $\mu \gg T$, as (5.40) would not be valid, and the presence of large derivatives of μ may slow down the cooling. However, it is reasonable to assume that for a time of $t \sim 10^{-4}$ s, which is five orders of magnitude larger, the temperature will be of the order $T_0/3$ or smaller. This, as will be discussed below, will imply that the object falls in the CFL phase [24]-[25].

All the previous approximation is assumed to be valid for small chemical potential $\mu \ll T$. By taking into account (3.23) and by neglecting the surface term, it follows that

$$R^3 \mu^2 T = 3\pi^4 R_0^2 T_0^2.$$

This suggest that the regime $\mu \sim T$ is achieved for some radius R_1 and some temperature and chemical potential $\mu_1 \simeq T_1$ such that

$$R_1 T_1 \sim (R_0 T_0)^{\frac{2}{3}}.$$

Since initially $R_0 T_0 \sim 10^{13}$, it is seen that now $R_1 \mu_1 \sim 10^{10}$. If the temperature is not significantly changed, then this implies that there is a violent contraction to $R_1 \sim 10^{-2} - 10^{-3}$ cm and the chemical

potential reaches the value $\mu \sim 100$ MeV. In order to check if this is true note that, at initial stages, the dominant term in the right hand side of (3.18) is the one proportional to the surface tension σ . In this equation, this term dominates the emissivity, whose maximum value corresponds to $T \sim 100$ MeV and $R \sim 1$ cm. If all the non relevant terms are neglected in (3.18) the equation simplifies to a Newtons law equation of the form

$$R^2 \ddot{R} \sim -2R.$$

The integration of this equation gives that

$$\frac{\sqrt{\pi} R_0}{2} \text{Erf}\left(\sqrt{\log \frac{R_0}{R}}\right) \sim t.$$

Here $\text{Erf}(x)$ is the error function. For a contraction of $R = 10^{-3} R_0$, this gives around $t \sim 10^{-10}$ s. However, these arguments have a problem, as the velocity of the wall is given by

$$\dot{R}^2 = -4 \log \frac{R}{R_0}.$$

If this expression is taken literally into account, then contraction velocity reaches a superluminal value $\dot{R}^2 > 1$ at some point. This suggests the the bubble surface may reach velocities close to light, and the non relativistic approximation employed here is not valid. However, assume that the bubble wall moves with light velocity. Then, it makes around 10^9 m per second, which means that it travels a distance of the order of centimeter with a time around $t \sim 10^{-11}$ s. All the previous discussion suggests that a contraction from R_0 to $R = 10^{-3} R_0$ occurs in a time of the order $t \sim 10^{-9} - 10^{-11}$ s. In this period μ reaches the value $\mu \sim T_0$ and, as the process seems to be very quickly, it is plausible that no significant cooling takes place during this contraction. Thus, at the end $\mu \sim T_0 \sim 100$ MeV.

Once the chemical potential reaches the value $\mu \sim 100$ MeV, there is a further period of contraction in which the chemical potential grows. In order to see this, note that for $\mu \gg T_0$ the conservation of baryon number (3.23) gives that

$$\mu \sim 2 \frac{(R_0 T_0)^{\frac{2}{3}}}{R}. \quad (5.41)$$

The last formula shows that $\mu = \mu(R)$, and it is independent on the value of T . On the other hand, the right side of (3.18) can be approximated as

$$\begin{aligned} \Delta P = & -8\pi\sigma R + 4\pi R^2 \frac{7}{8} \frac{\pi^2 g T^4}{90} \left(1 + \frac{30\mu^2}{7\pi^2 T^2} + \frac{15\mu^4}{7\pi^4 T^4}\right) - 4\pi R^2 E_B \Theta(\mu - \mu_1) \left(1 - \frac{\mu_1^2}{\mu^2}\right) \\ & - 4\pi R^2 \frac{7}{8} \frac{\pi^2 g T_e^4}{90} + F_\eta \sim -8\pi\sigma R + \frac{g}{12\pi} \frac{2^4 (R_0 T_0)^{\frac{8}{3}}}{R^2}. \end{aligned}$$

In making this approximation, the term proportional to μ^4/T^4 was assumed to be leading, and the formula (5.41) was employed for replacing μ as a function of R . This term clearly is larger than μ^2/T^2 and than one. The terms proportional to $E_B \sim (150 \text{ MeV})^4$ and to T_e are also small in comparison with $\mu \gg 100$ MeV, for a radius smaller than a centimeter. Now, if the object is assumed to enter in the CFL phase, the emissivity may be neglected. The equilibrium position R_e is then the zero of the last expression and, with the present choice of parameters, is given by

$$R_e \sim 4 \cdot 10^{-6} \text{ cm}.$$

A further comment about this magnitude is in order. The surface tension σ of the domain wall, as discussed in (2.4), is $\sigma \sim 10^{20} \text{ MeV}^3$. However, for small bubbles, a radial dependence $\sigma = \sigma(R)$ may appear. In obtaining this number, we have assumed that $\sigma \sim 10^{19} \text{ MeV}^3$, that is an order of magnitude less than the original value. This difference does not change significantly the equilibrium radius R_e , it simply corrects it by a factor of two.

The chemical potential μ that follows from (5.41) is indeed very large, $\mu > 500$ MeV. Thus the hypothesis that the emissivity can be safely omitted is reasonable. In these terms, one has from (3.13) that at the end of the evolution one has from $M \sim 10^{32}$ MeV. The baryon number is $B \sim 10^{29}$. This leads to an energy per baryon $M/B \sim \text{GeV}$, which is of the order of a typical nucleon m_N formed during that epoch. This is a condition for warrant the stability of the object [2].

The linealization of (3.18) around this equilibrium position R_e gives

$$\delta\ddot{R} + \frac{2}{\tau}\delta\dot{R} + \omega^2\delta R = 0.$$

This equation corresponds to exponentially damped oscillator with characteristic time scale τ and frequency ω^2 which, in this case, are given by

$$\tau \sim \frac{10\pi\sigma R_e}{3\eta}, \quad \omega^2 \sim \frac{18}{5R_e^2}.$$

With the values employed in this section, it follows that $\tau \sim 10^{-4} - 10^{-3}$ s and $\omega\tau \sim 10^{13} \sim m_\pi/m_a$. This implies that the external temperature T_e in (3.15) is close to $T_e \sim T_0/\sqrt{10} \sim T_0/3$. Thus, it is plausible that the external temperature when the object is formed is close to the value $T \sim 41$ MeV, a number that have several interesting phenomenological consequences.

The value of R_e obtained here is two or three orders of magnitude smaller than the one obtained in [1], but the value of σ employed here is two of three orders of magnitude larger. This implies that the time of formation τ is approximately the same of that reference. It should be remarked however, that the value of η was calculated by assuming baryon number equal to zero, thus a more precise knowledge of this coefficient of course is desirable.

6. Viability of axion nuggets as dark matter candidates

In the present work, the formation of axion quark nuggets and their possible evolution was analysed, but taking into account a large emission of neutrinos inside the object. As a result, the final radius of the object is smaller than the one predicted in [5]. However, the analysis done here employs a smaller axion mass and the time of formation of the object remains basically the same as in [1]. The universe external temperature at the formation time is around $T_f \sim 41$ MeV. The importance of this value is the following [2]. The baryon to photon density that is currently available is

$$\eta \sim \frac{n_B - \bar{n}_B}{n_\gamma} \sim 6 \cdot 10^{-10}.$$

This value can be estimated as $\eta \sim T_{eq}/m_N$ between the temperature $T_{eq} \sim 1$ eV of equilibrium between radiation and matter. Here m_N is a typical nucleon mass, which, in order to reproduce the observations, should be $m_N \sim 1$ GeV. On the other hand, at the time of formation $n_B - \bar{n}_B \sim n_B \sim e^{-\frac{m_N}{T_f}}$. The value $T_f \sim 41$ MeV is the one consistent with the measurements of the parameter $\eta \sim 6 \cdot 10^{-10}$. For this reason, the possibility that these objects are a considerable fraction of dark matter and may contain a large number of anti-baryon number, consistent with the measured baryon-anti baryon asymmetry, remains plausible.

There are several consistency checks that these objects should fulfill in order to classify as cold dark matter candidates [1]-[14]. It is important to see if these conditions are satisfied by the objects described in the present work. The first condition is that these objects should be long lived. By assuming a geometric cross section, the total number of collisions between ordinary hadrons and axion quark nuggets is given by

$$\frac{dW}{dt} = 4\pi R^2 n_B v, \quad n_B \sim \frac{0.15\rho_{dm}}{\text{GeV}}.$$

From here it follows that the annihilation of baryon charge until the present time is

$$\Delta B = \frac{1}{H} \frac{dW}{dt}.$$

By employing a age of the universe of the order $t_u \sim 10^{17}$ s, a typical hadron velocity $v \sim 10^{-3}$ and the formation size of the object $R_e \sim 10^{-5}$ cm, it follows that $\Delta B \sim 10^{17}$, which is a value less than the value $B \sim 10^{28} - 10^{29}$ employed here. For larger values of R_e and B , the same conclusion holds. Thus, these objects have a life time larger than the universe age.

Another important aspect is the ratio between the energy density contribution of quark nuggets and ordinary baryons [3]. If one assumes that these nuggets are the most important component of dark matter, then the excess of anti-baryons is hidden inside these compact objects and is of the order of the baryon excess

$$\bar{n}_{\text{dm}} - n_{\text{dm}} = \frac{1}{B}(n_B - \bar{n}_B) \sim \frac{n_B}{B}.$$

By assuming that the excess of anti-nuggets is of the same order than the number of nuggets and anti-nuggets, one has then that $n_{\text{dm}} + \bar{n}_{\text{dm}} = C(\bar{n}_{\text{dm}} - n_{\text{dm}})$ with $C \geq 1$. This, combined with the previous relation, gives that

$$\frac{\bar{n}_{\text{dm}} + n_{\text{dm}}}{n_B} = \frac{C(\bar{n}_{\text{dm}} - n_{\text{dm}})}{n_B} = \frac{C}{B}.$$

In these terms it follows that

$$\frac{\Omega_{\text{dm}}}{\Omega_B} \sim \frac{m_{\text{qn}}(\bar{n}_{\text{dm}} + n_{\text{dm}})}{m_N n_B} \sim \frac{C m_{\text{qn}}}{B m_N}. \quad (6.42)$$

By taking into account that $m_{\text{qn}} \sim B m_N$, one has that $\Omega_{\text{dm}} \geq \Omega_B$, within a magnitude order. This is an interesting feature, since this relation is difficult to establish for models of dark matter not related to ordinary quark or baryon degrees of freedom [3].

It should be emphasised that the axion quark nuggets do interact with photons [6]. However, this does not pose a problem for being cold dark matter candidates if the mean free time for a photon to encounter a nugget is larger than the age of the universe. The mean free time for photons to collide with a nugget is given by $t_h = (n_B \sigma)^{-1}$, where the cross section σ is assumed to be the geometric one $\sigma = 4\pi R_e^2$. A convenient way to estimate t_h is to consider the mean free path for a photon before colliding with a baryon. This is given by [15]

$$t_b = \frac{1}{x_e n_B \sigma_T} \sim 3.9 \cdot 10^{18} \frac{a^3}{\Omega_B h^2} s,$$

with x_e the fraction of ionised particles and σ_T the Thompson cross section for baryons. Thus

$$t_h \sim \frac{\sigma_T}{4\pi R^2} \frac{n_B}{n_{\text{dm}}} 3.9 \cdot 10^{18} \frac{a^3}{\Omega_B h^2} s.$$

This can be expressed in terms of $\Omega_{\text{dm}} h^2$ by use of (6.42) as follows

$$t_h \sim \frac{\sigma_T}{4\pi R^2} 3.9 \cdot 10^{18} \frac{a^3}{\Omega_{\text{dm}} h^2} s \frac{m_{\text{dm}}}{m_N}.$$

On the other hand, at the time of matter radiation equality

$$a_{eq} \sim \frac{4.15 \cdot 10^{-5}}{\Omega_m h^2} \sim 3.5 \cdot 10^{-4}, \quad T_{eq} \sim 5.7 \Omega_m h^2 \text{eV} \sim 0.73 \text{eV},$$

where the estimation $\Omega_m h^2 \sim 0.128$ has been employed. As $a \sim T^{-1}$ it follows that

$$a \sim \frac{2.55 \text{ eV}}{T} 10^{-4}.$$

By taking into account that $\sigma_T \sim 2.4\pi m_N^{-2}$, that $R_e \sim 10^{-5}$ cm and that $m_{\text{dm}} \sim m_N B$, it follows that

$$t_h \sim \frac{10^{17}}{\Omega_{\text{dm}} h^2} \left(\frac{2.55 \text{eV}}{T} \right)^3 s.$$

Here the value $B \sim 10^{29}$ was employed, which corresponds to $R_e \sim 10^{-5}$ cm. This time is larger than the Hubble time

$$H^{-1} \sim 1.13 \cdot 10^{12} \left(\frac{\text{eV}}{T} \right)^{\frac{3}{2}} \frac{s}{\sqrt{\Omega h^2}},$$

thus the axion quark nuggets may be considered components of cold dark matter even when they strongly interact with light. In other words, it takes really a long time for a photon for reaching the compact object.

The tests given above suggest that these objects are a viable candidate for cold dark matter. Further cosmological applications such as the ones discussed in [1]-[14] will be considerate in a separate work.

Acknowledgments

O. S is supported by CONICET, Argentina.

References

- [1] A. Zhitnitsky JCAP 0310 (2003) 010.
- [2] D. Oaknin and A. Zhitnitsky Phys.Rev. D71 (2005) 023519.
- [3] A. Zhitnitsky Phys.Rev. D 74 (2006) 043515.
- [4] K. Lawson and A. Zhitnitsky Phys. Lett. B 724 (2013) 17.
- [5] K. Lawson and A. Zhitnitsky Phys. Rev. D 95 (2017) 063521.
- [6] X. Liang and A. Zhitnitsky Phys. Rev. D 94 (2016) 083502.
- [7] S. Ge, X. Liang and A. Zhitnitsky Phys. Rev. D 97 (2018) 043008.
- [8] A. Zhitnitsky Physics of the Dark Universe 22 (2018), 1
- [9] K. Lawson and A. Zhitnitsky Physics of the Dark Universe (2019) 100295.
- [10] N. Raza, L. van Waerbeke and A. Zhitnitsky Phys. Rev. D 98 (2018) 103527.
- [11] H. Fischer, X.Liang, Y. Semertzidis, A. Zhitnitsky and K. Zioutas Phys. Rev. D 98 (2018) 043013.
- [12] L. van Waerbeke and A. Zhitnitsky Phys. Rev. D 99 (2019) 043535.
- [13] V. Flambaum and A. Zhitnitsky Phys. Rev. D 99 (2019) 043535.
- [14] S. Ge, K. Lawson and A. Zhitnitsky Phys. Rev. D 99 (2019) 116017.
- [15] E. Kolb and M. Turner The Early Universe (Addison-Wesley, 1990).
- [16] A. Sakharov Soviet Physics Journal of Experimental and Theoretical Physics (JETP) 5 (1967) 24.

- [17] A. Sakharov Soviet Physics Uspekhi 34 (1991) 392.
- [18] R. D. Peccei and H. R. Quinn, Phys. Rev. D 16 (1977) 1791; S. Weinberg, Phys. Rev. Lett. 40 (1978) 223; F. Wilczek, Phys. Rev. Lett. 40 (1978) 279.
- [19] J.E. Kim, Phys. Rev. Lett. 43 (1979) 103; M.A. Shifman, A.I. Vainshtein, and V.I. Zakharov, Nucl. Phys. B166 (1980) 493.
- [20] M. Dine, W. Fischler, and M. Srednicki, Phys. Lett. B104 (1981) 199; A.R. Zhitnitsky, Yad.Fiz. 31 (1980) 497; Sov. J. Nucl. Phys. 31 (1980) 260.
- [21] P. Sikivie Lect. Notes Phys. 741 (2008) 19.
- [22] T.W.B. Kibble, J. Phys. A9 (1976) 1387; W. Zurek, Nature 317 (1985) 505.
- [23] W. Zurek, Phys. Rep. 276 (1996) 177.
- [24] M. Alford, K. Rajagopal, T. Schäfer and A. Schmitt Reviews of Modern Physics. 80 (2008) 4.
- [25] M. Alford, K. Rajagopal and F. Wilczek Physics Letters B. 422 (1998) 247.
- [26] A. R. Bodmer, Phys. Rev. D4 (1971) 1601.
- [27] E. Witten Phys. Rev. D 30 (1984) 272. .
- [28] A. Atreya, A. Sarkar. and A. Srivastava Phys. Rev. D 90 (2014) 045010.
- [29] J. Preskill, M. Wise and F. Wilczek, Phys. Lett. B 120 (1983) 127; L.Abbot and P. Sikivie, Phys. Lett. B120 (1983) 133.
- [30] M. Dine and W. Fischler Phys. Lett. B 120 (1983) 137.
- [31] D. Dicus, E. Kolb, V. Teplitz and R. Wagoner, Phys. Rev. D 18 (1978) 1829.
- [32] I. Chen and E Nakano. Phys. Lett. B 647 (2007) 371.
- [33] V. Petrosian, G. Beaudet and E. Salpeter Phys. Rev. 54 (1967) 1445.
- [34] N. Iwamoto Phys. Rev. Lett 44 (1970) 1637.
- [35] N. Iwamoto Annals of Physics 141 (1982) 1.
- [36] N. Iwamoto Phys. Rev. D 28 (1983) 2353.
- [37] B. Datta, S. Raha and B. Sinha Mod. Phys. Lett A Vol 3 Num 14 (1988) 1385.
- [38] A. Goyal and S. Dutta Phys. Rev. D 49 (1994) 3910.
- [39] S. Adhya Advances in High Energy Physics Volume 2017 (2017) 127393
- [40] T. Tatsumi and T. Muto Phys. Rev. D 89 (2014) 103005.
- [41] Q. Wang, Z. Wang, J. Wu Phys.Rev. D74 (2006) 014021.
- [42] L. Masperi and M. Orsaria Part. Nucl. Lett. 1 (2004) 80.
- [43] J. Horvath and H.Vucetich Phys.Rev. D59 (1999) 023003.
- [44] S. Reddy, M. Sadzikowski and M. Tachibana Nucl. Phys. A 714 (2003) 337.

- [45] V. Gupta, A. Adhwa and J. Anand Pranama Journal of Physics 45 (1995) 195.
- [46] P. Jaikumar, C. Roberts and A. Sedrakian Phys. Rev. C 73 (2006) 042801.
- [47] D. Yakovlev, A. Kaminker, O. Gnedin and P. Haensel Phys. Rept. 354 (2001) 1.
- [48] D. Blaschke, H. Grigorian and D. N. Voskresensky Astron. Astrophys. 424 (2004) 979.
- [49] D. Blaschke and J. Berdermann "Neutrino emissivity and bulk viscosity of iso-CSL quark matter in neutron stars" Proceedings of QCD Workshop 2007, Martina Franca (Italy).
- [50] J. Berdermann, D. Blaschke, T. Fischer and A. Kachanovich Phys. Rev. D 94 (2016) 123010.
- [51] D. Blaschke, T. Klaehn and D. Voskresensky Astrophys. J. 533 (2000) 406.
- [52] D. Blaschke, H. Grigorian and D. Voskresensky Astron. Astrophys. 368 (2001) 561.
- [53] D. Blaschke, H. Grigorian and D. Voskresensky Astron. Astrophys. 424 (2004) 979.
- [54] J. Berdermann, D. Blaschke, H. Grigorian and D. Voskresensky Progress in Particle and Nuclear Physics 57 (2006) 334.
- [55] D. Blaschke, H. Grigorian, D. Voskresensky and F. Weber Phys.Rev. C 85 (2012) 022802.